THE USE OF NUMERICAL ANALYSIS TO AID THE DESIGN OF MONOPILE FOUNDATIONS FOR A NORTH SEA OFFSHORE WIND FARM

Felix C. Schroeder, Geotechnical Consulting Group, London, UK, f.c.schroeder@gcg.co.uk
Angeliki Grammatikopoulou, Geotechnical Consulting Group, London, UK, a.grammatikopoulou@gcg.co.uk
Andy Barwise, Innogy Renewables UK Ltd, andy.barwise@innogy.com
Stephen MacKinnon, Innogy Renewables UK Ltd, strephen.mackinnon@innogy.com
Richard J. Jardine, Imperial College London, UK, r.jardine@imperial.ac.uk
David M. Potts, Imperial College London, UK, d.potts@imperial.ac.uk

ABSTRACT

This paper outlines the application and extension of the recently proposed PISA design approach, to support foundation design for the Triton Knoll array of monopile supported wind-turbine generators, which are sited off the UK's east coast and will deliver 855 MW from 2021. Emphasis is placed first on the site characterisation employing in-situ profiling and advanced laboratory testing that allowed location-specific, locally calibrated, 3D FE analyses with the Imperial College Finite Element Code ICFEP. The analyses recognised the small strain stiffness and yielding behaviours of the generally dense sands and stiff glacial till units encountered. The ability of the chosen constitutive models to accurately replicate the most critical features of soil response is demonstrated by comparing single element FE analyses with laboratory test data. Examples are then shown from the comprehensive sets of 3D monopile analyses undertaken of a static loading case that provided predictions for ultimate and service limit states and allowed the extraction of soil reaction curves for use in further design optimisation. The advanced site characterisation and numerical analysis enabled the foundation designers to achieve substantial savings in the project's foundations' capital costs.

Keywords: monopile foundations, finite element analysis, constitutive modelling

INTRODUCTION

The Triton Knoll (TK) array of ninety 9.5MW monopile supported wind turbine generators (WTGs) is being constructed 20 miles off the east coast of Lincolnshire in England (see Fig. 1) and will deliver 855 MW from 2021 onwards. Given the relatively large proportion of the project's capital cost invested in its foundations, efficient design of TK's 90 monopiles in water depths of up to 31m was central to the project's success. Monopile foundations, with large lateral and moment loading capacities, often offer efficient design solutions and have been adopted for most offshore WTGs installed to date. There has been a progressive trend over the last decade towards installing ever larger diameter monopiles, usually with ever lower length-to-diameter (*L/D*) ratios and in often ever greater water depths. The design of offshore piles to resist lateral and moment loads is frequently based on calculations undertaken using non-linear Winkler p-y curves employed in beam-spring analyses. The p-y curves specified by API (2011) are still commonly employed for sand and clay sites. These expressions are relatively easy to use and only require basic soil parameters, such as undrained strengths in clay deposits and angles of shearing resistance in sands. However, foundation monitoring, including that undertaken previously at the Magnus and Hutton TLP oil production platforms showed that the traditional p-y (lateral) and t-z (axial) procedures can greatly under-estimate the true vertical, horizontal and moment stiffness developed by large piles driven in very stiff North Sea tills and dense sands. Far better Class A predictions (i.e. made before the field measurements, Lambe, 1973) were obtained for these sites by performing finite element (FE) analyses with the Imperial College code ICFEP (Potts & Zdravković, 1999) that recognised and

modelled, the soils' small strain and yielding behaviour seen in advanced laboratory tests on high quality samples (see Jardine and Potts (1988 & 1993), Kinley & Sharp (1993)).

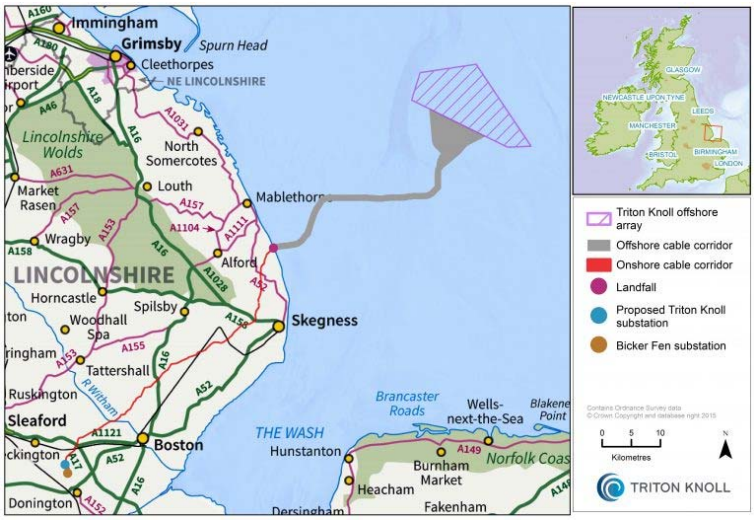

Fig. 1. Location of Triton Knoll Offshore Wind Farm (from www.tritonknoll.co.uk)

The recent PISA and PISA2 JIPs (e.g. Byron et al., 2019) developed new design methodologies tuned specifically to model monopile foundations. The key components comprise: (i) accurate characterisation of ground conditions that enables the use of representative constitutive soil models, (ii) advanced 3D FE analyses conducted with ICFEP and (iii) development from these analyses of four sets of calibrated soil reaction curves that can be applied in the large numbers of optimisation calculations required during the monopile design process for an OWF. The methods' ability to deliver greatly improved predictions for monopile response under lateral and moment loading was demonstrated by the close agreement achieved between Class A predictions and the outcomes of large-scale field experiments conducted in glacial clay tills and sands as part of the PISA programme.

This paper describes how the PISA methodology was applied at a relatively early stage of the TK OWF design process in order to guide the detailed design of monopiles for each WTG. It summarises the work undertaken to characterise the soils encountered, calibrate the constitutive models employed and undertake comprehensive 3D ICFEP analyses to assess the monopiles' performance under static lateral and moment loading conditions. Cyclic loading conditions were also considered through the explicit modelling of individual load cycles to determine the expected damping behaviour and the use of a numerical procedure which enables the determination of permanent deformation for given design storms. Due to space restrictions, the cyclic loading laboratory testing and analyses are not reported in this paper.

GROUND CONDITIONS, MATERIAL MODELS AND ASSOCIATED PARAMETERS

The Triton Knoll OWF project area is characterised by Quaternary sediments of varying thickness. The dominant Pleistocene deposits were deposited in alternating glacial and interglacial cycles, resulting in over-consolidated clays and dense sands. This paper illustrates the modelling undertaken by considering the example of an approximately 7m diameter monopile with an embedment depth of 21m at a location comprising the following geotechnical formations:

- **Holocene deposits;** assumed to be removed by scouring following monopile installation (less than 1.3m thick).
- **Bolders Bank Formation (BDK)**; an ablation till (primarily overconsolidated, ductile, low plasticity clays) deposited during the Weichselian glacial period.

- **Egmond Ground Formation (EG)**; dense to very dense very gravelly coarse sand deposited in high energy marine conditions during the Holsteinian period.
- **Sand Hole Formation (SH)**; a large variety of materials, ranging from clayey silty sand with widely spaced beds of clay to very high strength clay with widely spaced beds of medium dense sand, deposited in estuarine/intertidal and glaciomarine/ marine environments during the Elsterian period.
- **Swarte Bank Formation (SBK)**; channel infill materials deposited in lacustrine to shallow marine interglacial conditions, which can be separated into three principal units comprising subglacial tills, glaciofluvial material and laminated glaciomarine clays, with the basal till unit thought to contain a high proportion of reworked chalk.

The idealised stratigraphy is indicated on the CPTu profile given in Fig. 2; 10m of BDK is underlain by 6.5m of EG, 11m of SH and an assumed 7.5m of SBK overlying basal chalk. The modelling of each main formation was undertaken on the basis of site-specific advanced laboratory testing undertaken by Fugro on samples from across the windfarm area and applied to specific locations on the basis of CPT profiling at each turbine position.

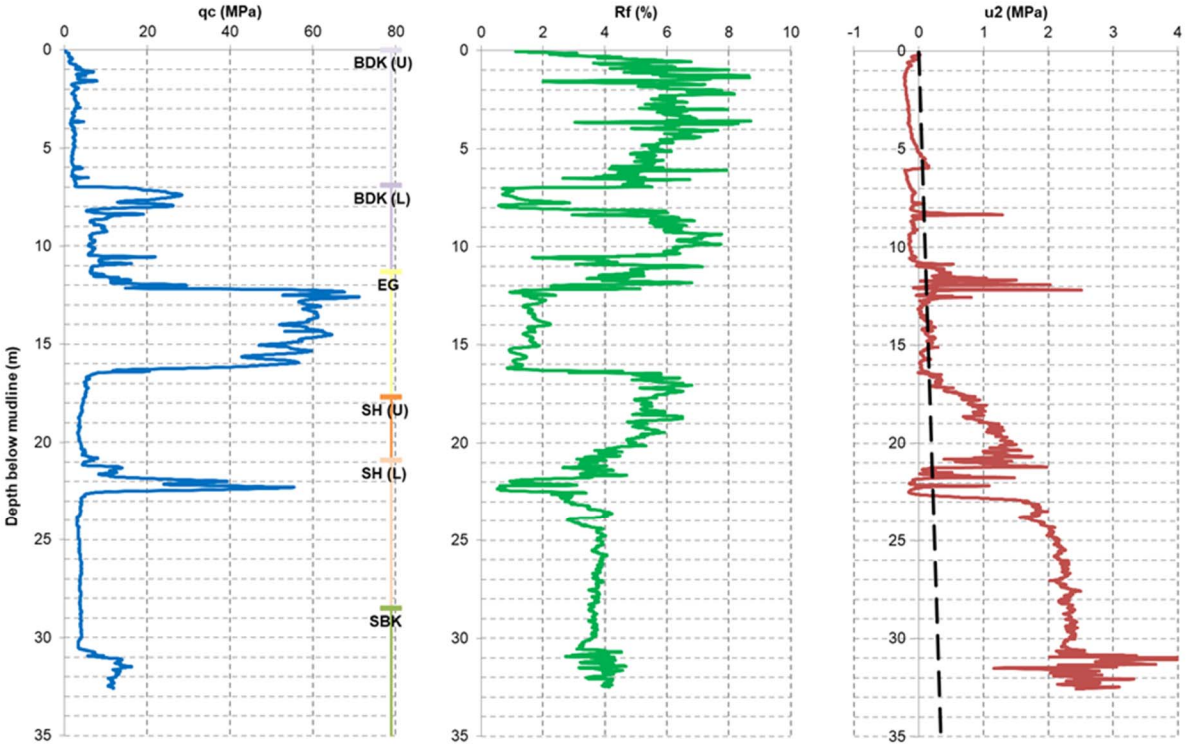

Fig 2. CPT profile and assumed stratigraphy

Bolders Bank Formation (BDK) and other clay units (SH and SBK)

The PISA JIP programme addressed the behaviour of clay tills by conducting laboratory and in-situ soil testing at Cowden, where the till section concerned is a member of the BDK formation. The experimental data collected across the Triton Knoll project area indicated that the members present at TK should be split into upper and lower sections, BDK(U) and BDK(L), with the latter being generally stiffer and stronger.

Both BDK sections were modelled for TK as in the PISA JIP analyses reported by Zdravkovic et al. (2019), employing an extended Modified Cam Clay (MCC) model available in ICFEP with stress and strain dependent non-linear pre-yield behaviour, a non-linear Hvorslev surface on the dry side and a general shape for the yield and plastic potential surfaces in the deviatoric plane. The MCC compressibility parameters, λ, κ and v_1 were derived from 9 oedometer tests

on BDK(U) samples and 5 on BDK(L) specimens. Undrained triaxial compression and extension tests were analysed to establish critical state angles of shearing resistance, φ'_{cs} (see Fig. 3a) and define a realistic variation of φ'_{cs} with Lode's angle, θ (see Fig. 3b).

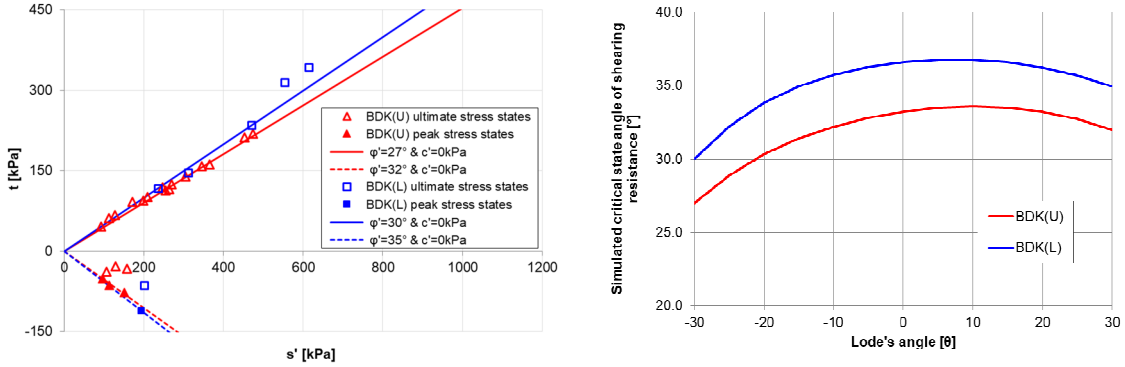

a) **b)**

Fig. 3. Determination of critical state parameters (φ'_{cs}) for BDK(U) and BDK (L) layers a) Drained triaxial test data and b) Assumed variation of φ'_{cs} with Lode's angle

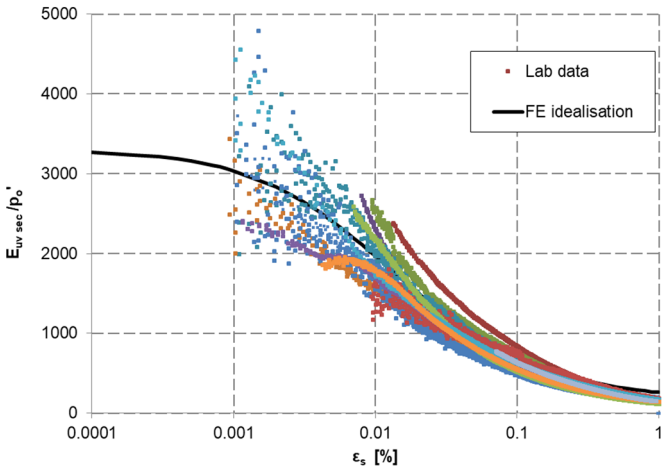

Fig. 4. Derivation of stiffness-strain curve on the basis of laboratory test data for BDK(U)

Figure 4 shows the variation of normalised secant undrained Young's moduli, E_u, with shear strain invariant, ε_s, obtained from undrained triaxial compression tests on BDK(U) employing local axial strain measurements (where ε_s is equal to axial strain in undrained triaxial tests). Isotropic small strain stiffness modelling was adopted in the analyses, in line with the PISA analyses performed for the Cowden monopile tests (see Zdravkovic et al. 2019). The small strain stiffness overlay of Taborda et al. (2016) was coupled with the MCC formulation to reproduce stiffness non-linearity.

Undrained triaxial tests were simulated in single element FE analyses; the predictions for stress-strain, effective stress path, pore pressure-strain and stiffness-strain behaviours are compared with a typical CAUc triaxial compression test on overconsolidated till in Fig. 5, which shows ductile behaviour up to 30% strain. The initial K_0 values for these simulations were chosen to match the stress conditions of each sample at the beginning of undrained shearing. The assumed yield stress ratio, *YSR*, was chosen to replicate the undrained shear strength, S_u, measured in each test. The agreement between the simulation and the test data is excellent. A similar process was followed for the other clays identified in Fig. 2 (the BDK (L), SH and SBK units) to obtain site wide parameter sets in terms of the critical state and compressibility parameters and the parameters required to define the stiffness decay curves.

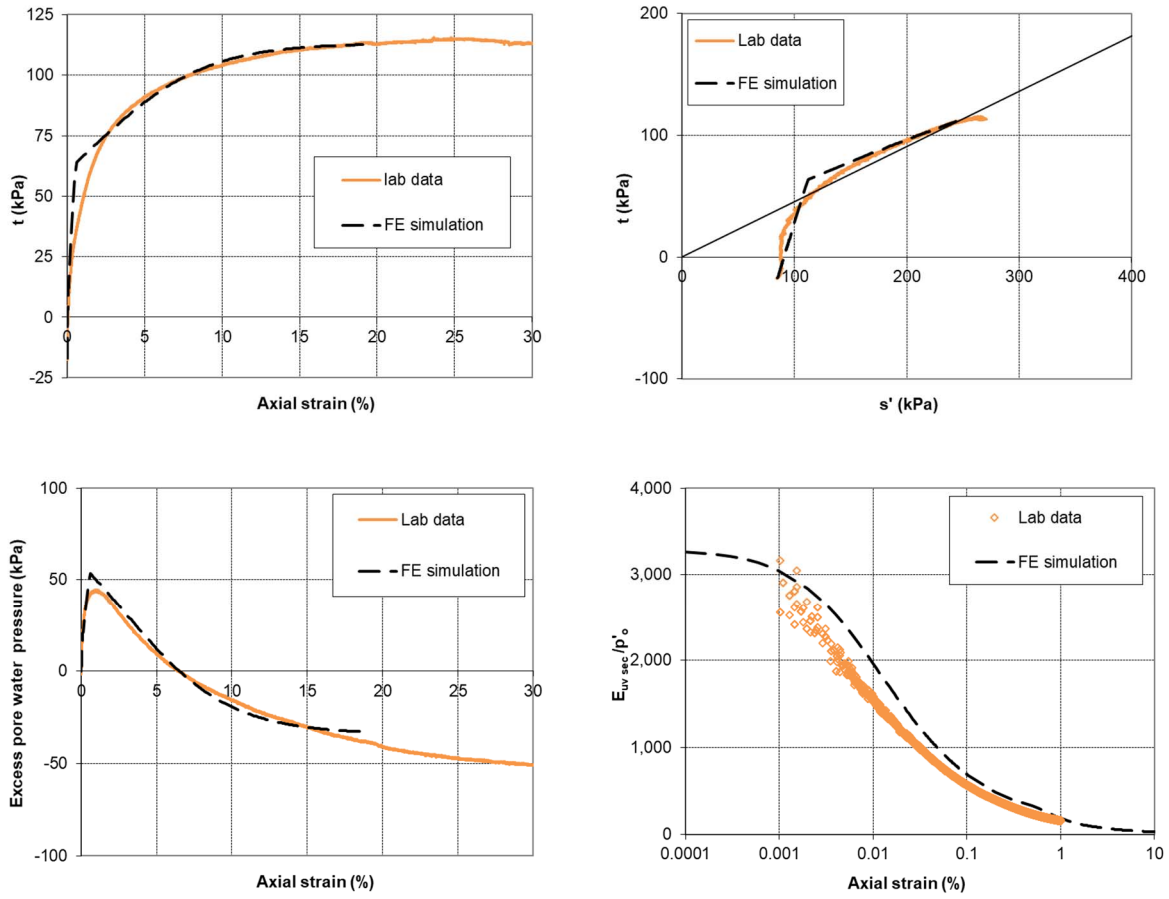

Fig. 5. Single element ICFEP simulation of CAUC test for BDK(U)

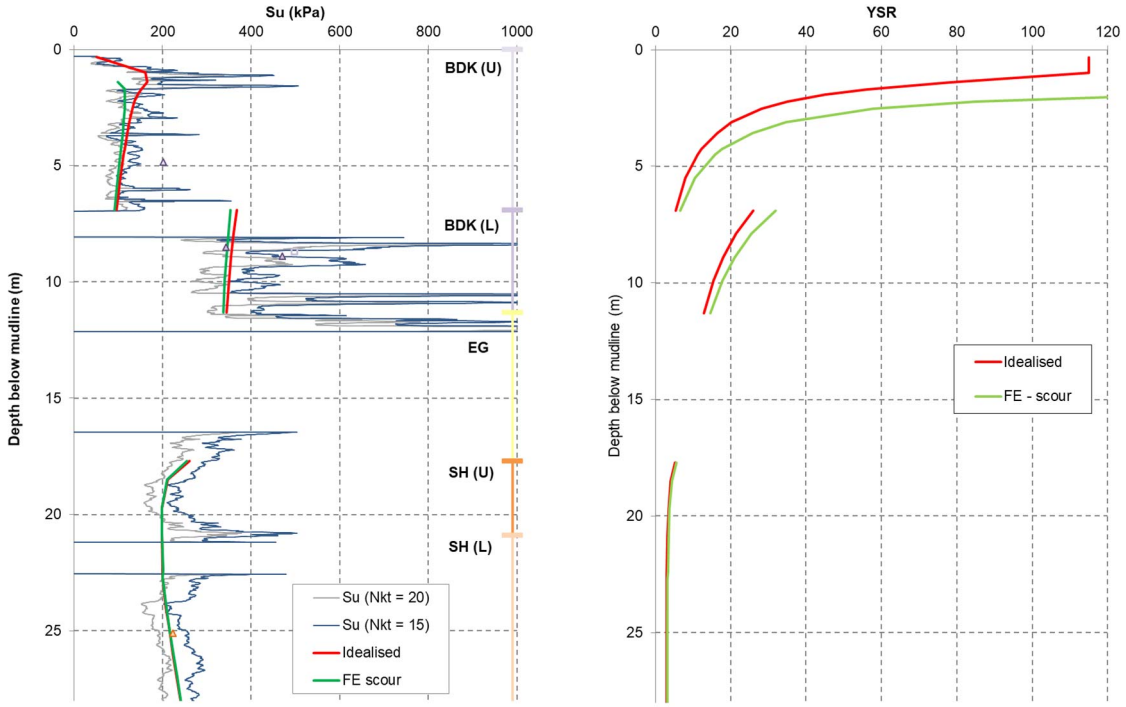

a) **b)**

Fig. 6. a) Undrained strength profile, and b) assumed YSR profile

A *YSR* profile with depth was then chosen for each location under consideration, to fit the location-specific undrained strength profile derived from the relevant CPT profile, which was made possible by the MCC formulation available in ICFEP. In this case, the undrained strength profile shown in Fig. 6a, derived from 'site-calibrated' N_{kt} values of 15 and 20, was matched using the *YSR* profile labelled as 'Idealised' in Fig. 6b. The FE calculations incorporated 1.3m of assessed scour by globally lowering the level of the original seabed, which is considered to be conservative. Consistent with the MCC model, this leads to changes in the undrained shear strength profile compared to that obtained from the unscoured CPT. Consequently, the profile applied in the analysis ('FE-scour' in Fig. 6) was derived by changing the initial vertical stress, as a result of global scour, and maintaining unchanged vertical yield stresses.

Egmond Ground Formation (EG)

The EG formation soils encountered at the example location comprise mainly very dense sands, as illustrated by the high q_c values in Fig. 2. Significant stress-strain peaks and markedly dilative behaviour were seen in isotropically consolidated drained (CID) triaxial tests on these materials, with the sands tending towards critical states at large strains. A strain softening variant of the Mohr-Coulomb model from ICFEP's extensive constitutive model library was chosen to represent this behaviour (see Grammatikopoulou et al. 2017) in which the angles of shearing resistance and dilation varied with plastic shear strain. Figure 7a shows the peak and critical state values obtained in multiple CID tests on EG sand samples. The figure also indicates the envelopes for the interpreted critical state angle of shearing resistance (33°) and peak angle of shearing resistance (43°) for triaxial compression. This is appropriate given the very dense conditions at the example WTG position under consideration.

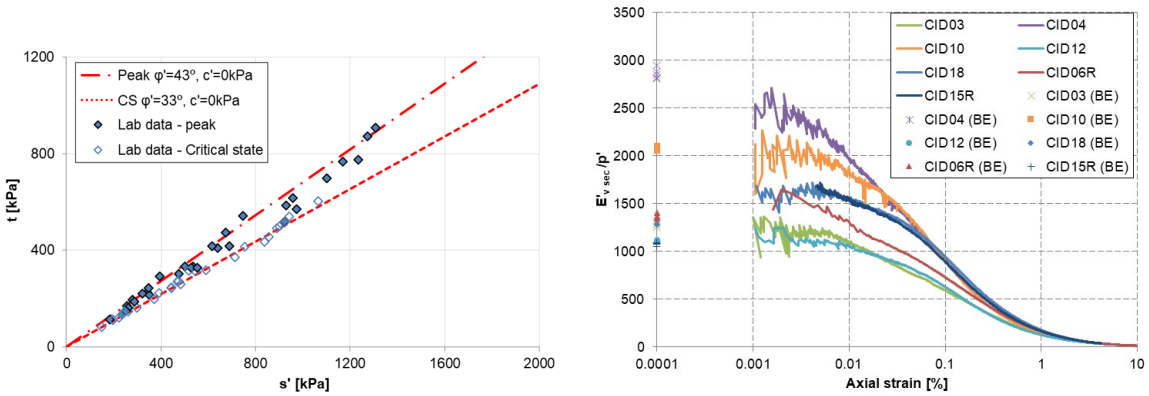

a) **b)**

Fig. 7. Determination of strength (a) and stiffness (b) parameters from CID tests on EG samples

The laboratory testing included CID tests, with pairs of local axial strain instruments, that were taken up to 30% axial strains. Bender element testing was also undertaken to determine G_{vh} values. The tests were carried out with different p' levels and initial relative densities (D_r = 60%, 75% and 90%) and covered overconsolidation ratios of 1.0 and 4.0 to capture the behaviour of the EG sands for a range of conditions. Figure 7b presents examples of the drained stiffness-strain curves obtained from these tests as normalised secant vertical Young's modulus, E', plotted against axial strain. Also shown are the G_{vh} bender element measurements plotted as E' assuming isotropic stiffness and a Poisson's ratio equal to 0.25. Part of the divergence seen in Fig. 7b between the seven high quality tests originates in the linear normalisation made by mean effective stress p'. It is generally accepted that the initial small strain stiffness of sands (G_0) depends on p' raised to a partial power of n, where n is approximately 0.5 over the range of interest; while for larger strains a linear normalisation with p' may be considered more appropriate. Based on the triaxial data and an interpretation of the CPT profile in Fig. 2 a $G_0/(p'^{0.5})$ ratio of 13,100 was determined. This was matched approximately over relevant depth

ranges in the FE analysis (see e.g. Schroeder et al., 2015) recognising the assumed linear normalisation with p' for all strain levels in the chosen pre-yield non-linear stiffness formulation.

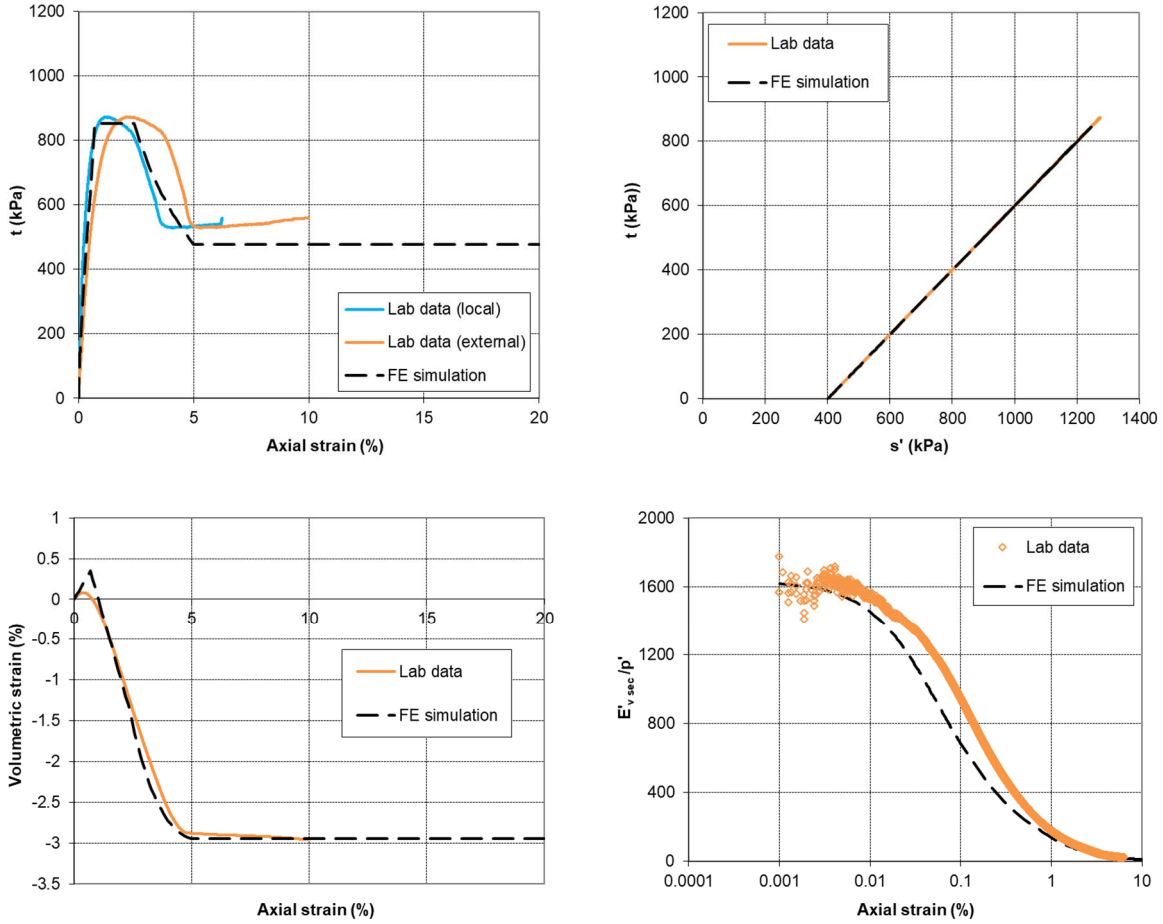

Fig. 8. Single element ICFEP simulation of CID test for EG

Figure 8 shows a single element simulation for a typical CID test on a very dense EG sample (representative of the EG materials encountered at the location considered in this paper), indicating very good agreement in all aspects of the stress-strain and volumetric response. The typical difference between the 'local' and 'external' stress-strain responses indicates the effect on the latter of bedding, tilting and compliance errors. The single element simulation aims to model the stiffer 'local' stress-strain response, which it captures representatively.

AN EXAMPLE OF THE 3D FE ANALYSES

The following sections illustrate the application of the adopted methodology to an approx. 7m diameter monopile with varying wall thickness of around 60mm, and a tip depth of around 21m below the scoured seabed, giving an *L/D* of around 3. Lateral loading was applied at around 42m above the scoured seabed. The FE mesh for the 3D ICFEP analyses extended to around 2*D* below the pile tip and out to a radius of 75m. High-order 20-noded hexahedral elements were used to discretise the soil domain in combination with 16-node interface elements (Day & Potts, 1994) along the monopile-soil interface and 8-node shell elements (Schroeder et al., 2007) to discretise the monopile.

Figure 9 shows the normalised load-displacement response expressed in terms of normalised lateral load (Fig. 9a) and the corresponding normalised secant lateral stiffness (Fig. 9b) plotted against mudline displacement. In terms of rotations, a mudline rotation of around 3 degrees was obtained for a mudline displacement of 10%D. The load in Fig. 9a was normalised by the

load for a mudline displacement of 10%*D* (a displacement that is commonly employed to represent failure conditions) and the secant stiffness in Fig. 9b was normalised by the initial value obtained from very small mudline displacements. Figure 9a suggests a ductile response with significantly higher lateral loads developing for displacements exceeding 10%D. Figure 9b highlights the highly non-linear nature of the global monopile response to lateral (and moment) loading with the analysis indicating a four-fold spread of operational stiffness for mudline displacements of up to 1%*D*.

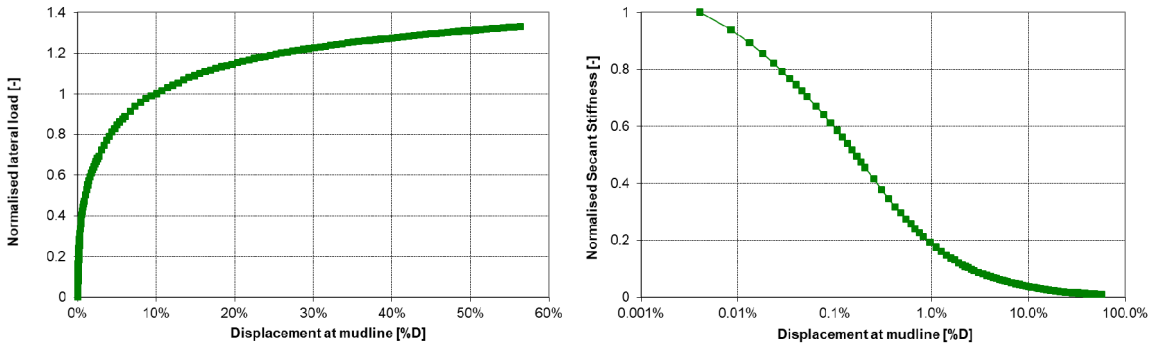

a) **b)**

Fig. 9. Monopile response to lateral and moment loading:
a) Normalised load-displacement curve and b) Secant stiffness-displacement response

The next step of the numerical approach in the PISA methodology is extraction from 3D FE analyses of the components necessary to define the following four soil reactions for application in simplified PISA 1D Winkler models:

1. Lateral load-displacement curves, distributed with depth down the monopile shaft
2. Similarly, distributed moment-rotation curves
3. A base shear-displacement curve, and
4. A base moment-rotation curve

The curves were derived from the results of ICFEP analyses by systematically extracting and integrating stress, nodal force and displacement data from the interface elements around the monopile, the shell elements of the monopile itself and the solid (soil) elements at the base of the pile. Figure 10a shows a selection of five lateral load-displacement curves extracted for varying depths, while Fig. 10b shows the base shear-displacement curve. Figure 11 shows the distributed lateral loads against depth below mudline for five mudline displacements.

The soil reaction curves show distinctly different patterns of behaviour in the clay till layers (BDK and SH) and the sandy EG stratum. The clay till (local) soil reaction curves all show ductile responses with relatively gentle build-ups of lateral resistance with increasing lateral displacement. In contrast, the displayed EG curve (at around 11.5m depth,) manifests a peak resistance after a local lateral displacement of around 5%*D*, after which the resistance reduces. This is further illustrated in Fig. 11 which shows a reduction in lateral resistance over the top part of the EG layer, where lateral displacements are largest. Figure 11 also shows how the soil profile variations translate into in the predicted patterns of local lateral resistance. It is also noticeable that the monopile's centre of rotation remains at around 14m depth, or 2/3 of the embedded length, throughout loading.

Examination of the normalised base shear response (see Fig. 10b) indicates effective mobilisation after relatively small local lateral displacements of approximately 1.5%*D*. The difference between the base shear and distributed lateral load responses in the SH stratum (the same material as at the base) are due to the different mechanism involved; while the base

shear results in a relatively thin shear zone, the lateral movement of the monopile engages far larger volumes of soil.

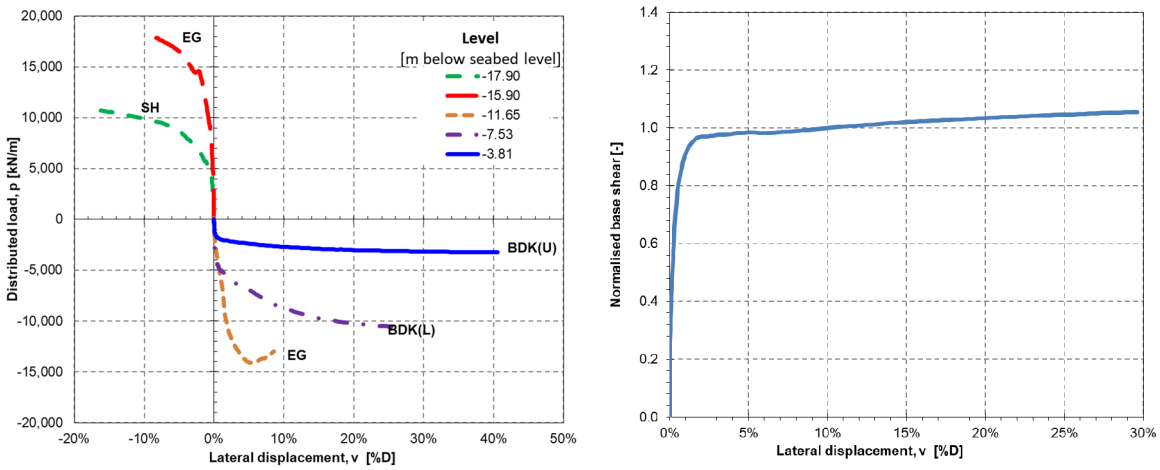

a) b)

Fig. 10. Soil-reaction curves extracted from FE analysis:
a) Example distributed lateral load-displacement curves and b) Base shear-displacement curve

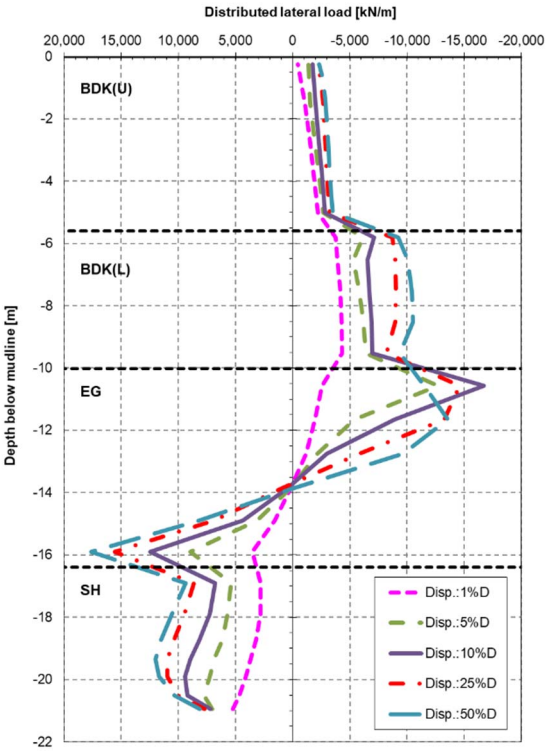

Fig. 11. Distributed lateral load plotted against depth for varying mudline displacement

CONCLUDING REMARKS

This paper demonstrates how the first critical steps of the PISA methodology have been applied as part of the monopile foundation design process for the UK Triton Knoll offshore wind farm. In the first instance careful characterisation of the ground conditions and soil mechanical behaviour was integrated with representative soil constitutive modelling through the ICFEP computational platform, showing excellent agreement between the observed and simulated soil behaviour. Subsequently, the 3D numerical model developed in ICFEP enabled derivation

of the four components of non-linear PISA soil reaction curves, which could then be applied in simplified PISA 1D Winkler modelling for multiple OWT locations across the TK wind farm site.

Although not presented herein, success in achieving more cost-effective foundation designs is confirmed independently by Manceau et al. (2019) who report ”implementation of improved soil response modelling based on the PISA JIP recommendations has led to a reduction of monopile embedment of 1 to 2 diameters compared to conventional design approaches based on historical p-y curves formulations. Compared to the trend of historical monopile foundations, the mass saving for the average hub height on the site is in excess of 30%”.

REFERENCES

American Petroleum Institute, API (2011). *Geotechnical and Foundation Design Considerations, API Recommended Practice 2GEO*, First Edition, April 2011.

Byrne, B.W., Houlsby, G.T., Burd, H.J., Gavin, K.G, Igoe, D., Jardine, R.J., Martin, C.M., McAdam, R.A., Potts, D.M., Taborda, D.M.G. and Zdravković, L. (2019). PISA design model for monopiles for offshore wind turbines: application to a stiff glacial clay till. *Géotechnique*, doi.org/10.1680/jgeot.18.p.255

Day, R.A. & Potts, D.M. (1994). Zero thickness interface elements – numerical stability and application. *Int. J. Num. Anal. Meth. in Geomechanics*, Vol. 18, No. 10, pp 689-708

Grammatikopoulou, A., Schroeder, F.C., Brosse, A.M., Andersen, K.W. and Potts, D.M. (2017). On the use of constitutive models in numerical analyses of offshore structures. *Proc. 8th SUT-OSIG Conference*, London, pp 423-430

Jardine, R.J. and Potts, D.M. (1988). Hutton Tension Leg Platform foundations: an approach to the prediction of driven pile behaviour. *Geotechnique*, 38(2), 231- 252.

Jardine R. J. & Potts D. M. (1993). Magnus foundations: Soil properties and predictions of field behaviour. *Proc. ICE Conf. Large scale pile tests in clay*, London, pp 69-83.

Kenley, R.M. & Sharp, D.E. (1993). Magnus foundation monitoring project instrumentation data processing and measured results. *Proc. ICE Conf. Large scale pile tests in clay*, London, 28-51.

Lambe, T.W. (1973). Predictions in soil engineering. *Geotechnique*, 23(2), 149-202.

Manceau, S., McLean, R., Sia, A. and Soares, M. (2019). Application of the Findings of the PISA Joint Industry Project in the Design of Monopile Foundations for a North Sea Windfarm. Offshore Technology Conference OTC 29557-MS

Potts, D.M. & Zdravković, L. (1999). Finite element analysis in geotechnical engineering: theory; Thomas Telford Publishing, London.

Schroeder, F.C., Day, R.A., Potts, D.M. & Addenbrooke, T.I. (2007). A quadrilateral isoparametric shear deformable shell element for use in soil-structure interaction problems. *ASCE Int. J. Geomechanics*, Vol. 7, No. 1, pp 44-52

Schroeder, F.C., Merritt, A.S., Sorensen, K.W., Muir Wood, A., Thilsted, C.L. & Potts, D.M. (2015). Predicting monopile behaviour for the Gode Wind offshore wind farm. Proc. Frontiers in Offshore Geotechnics, ISFOG III, Oslo, Norway

Taborda, D.M.G., Potts, D.M. & Zdravkovic, L. (2016). On the assessment of energy dissipation through hysteresis in finite element analysis. Computers & Geotechnics, 71, pp 180-194.

Zdravković, L., Taborda, D.M.G., Potts D.M., Abadias, D., Burd, H.J., Byrne, B.W., Gavin, K.G., Houlsby, G.T., Jardine, R.J., Martin, C.M., McAdam, R.A. and Ushev, R. (2019). Finite-element modelling of laterally loaded piles in a stiff glacial clay till at Cowden. Geotechnique, https://doi.org/10.1680/jgeot.18.PISA.005.